DOI: 10.1002/adma.200801178

High-Performance Liquid and Solid Dye-Sensitized Solar Cells Based on a Novel Metal-Free Organic Sensitizer**

By *Mingkui Wang, Mingfei Xu, Dong Shi, Renzhi Li, Feifei Gao, Guangliang Zhang, Zhihui Yi, Robin Humphry-Baker, Peng Wang,* Shaik M. Zakeeruddin,** and *Michael Grätzel**

Generating clean electricity with photovoltaic (PV) cells will make a big contribution to achieving sustainable energy supply on a global level.[1] It is well believed that the performance/price ratio will play a paramount role in the future choice of different PV devices. During the recent years, low-cost excitonic solar cells on the basis of organic optoelectronic materials have attracted considerable academic and industrial attention as potential candidates for the future PV market.[2] In the family of organic photovoltaic devices, the mesoscopic dye-sensitized solar cell (DSC) has achieved a validated 11.1% power conversion efficiency[3] and a remarkable long-term stability[4] under thermal and light-soaking dual stress, with polypyridyl ruthenium compounds as sensitizers.

Absorption of photons by an organic sensitizer will form an exciton or bound electron-hole pair[5] rather than the free charges normally produced in inorganic semiconductors. Contrary to other excitonic solar cells, due to the direct anchoring of a sensitizer onto the mesoporous wide-bandgap oxide semiconductors in DSCs, excitons are not required to diffuse toward an energy-offset hetero-interface to generate free charges at a yield close to unity, where the difference in the electron affinities between the contacting materials is large enough to overcome the exciton binding energy.[6] To intercept geminate charge recombination, the oxidized state of a sensitizer rapidly accepts an electron from a donor, most typically iodide in the electrolytes or transfers a hole to solid-state hole-transporting materials, efficiently regenerating its ground state. In a DSC, more critically, injected electrons need traverse a several micrometer thick semiconducting film usually consisting of interconnected titania nanocrystals, reaching the current collector before the occurrence of unwanted charge recombination with electron acceptors such as tri-odide in the electrolyte or holes in the solid-sate hole-transporting materials.[7]

In order to achieve a high optical absorption (η_A) and a qualitative charge collection yield (η_{cc}) simultaneously, the electron diffusion length (L_n) must exceed the optical absorption length (L_A) of the stained mesoporous film. DSCs employing solvent-free ionic liquid electrolytes or solid-state organic hole-transport materials, face the dilemma that L_A may become longer than L_n, entailing a loss in the photocurrent. Thus, it is imperative to develop new sensitizers with a high extinction coefficient to shorten the optical absorption length of the stained mesoscopic titania film. The dye should also exhibit a broad absorption to capture solar emission. Some organic sensitizers that possess high molar extinction coefficients seem to meet this requirement.[8] An impressive device efficiency up to 9% has been reached by employing an indoline dye along with an acetonitrile based electrolyte.[9] However, desorption of reported indoline dyes from the surface of TiO_2 adversely affected long-term stability. Inspiringly, ~6% stable devices have been achieved with a few organic senistizers such as a fluorene[10] or coumarin dye.[11]

To eliminate dye-desorption and enhance a long-term stability, we have designed and synthesized the novel organic sensitizer coded C201 which is shown in Figure 1. Importantly, this dye exhibits a low free energy of solvation in the high-polarity type electrolytes normally used in DSC, owing to the combination of fused thienothiophene and bisfluorenylaniline fragments. This sensitizer was synthesized in three steps at a very high yield. The Suzuki coupling of *N*,*N*-bis(9,9-dimethylfluoren-2-yl)-4-bromoaniline and thieno[3,2-*b*]thiophen-2-yl)boronic acid yielded 5-[*N*,*N*-bis(9,9-dimethylfluoren-2-yl)phenyl] thieno[3,2-*b*]thiophene, which was subsequently converted into its corresponding carbaldehyde via the Vilsmeier-Haack reaction. Finally, the aldehyde was condensed with cyanoacetic acid to give the target compound by means of the Knoevenagel reaction in the presence of piperidine. The detailed syntheses are described in the Supporting Information.

We employed square-wave voltammetry in combination with the ultramicroelectrode technique to measure the redox potentials of the C201 sensitizer. The negative offset of the

[*] Prof. P. Wang, M. Xu, D. Shi, R. Li, Dr. F. Gao, Dr. G. Zhang, Z. Yi
State Key Laboratory of Polymers and Chemistry
Changchun Institute of Applied Chemistry
Chinese Academy of Sciences (CAS)
Changchun, 130022 (China)
E-mail: peng.wang@ciac.jl.cn
Dr. S. M. Zakeeruddin, Prof. M. Grätzel, Dr. M. Wang
Dr. R. Humphry-Baker
Laboratory for Photonics and Interfaces
Swiss Federal Institute of Technology
1015 Lausanne (Switzerland)
E-mail: shaik.zakeer@epfl.ch; michael.graetzel@epfl.ch

[**] The National Key Scientific Program-Nanoscience and Nanotechnology (no. 2007CB936700), the National Science Foundation of China (no. 50773078), the Foundation for Outstanding Young Scientists of Jilin Province (no. 20070101), and the "100-Talent Program" of CAS are acknowledged for financial support. M. W., R. H.-B., S. M. Z., and M. G. thank the Swiss National Science Foundation for financial support. P. W. thanks EPFL for giving a visiting professorship. Supporting Information is available online from Wiley InterScience or from the authors.

ADVANCED MATERIALS

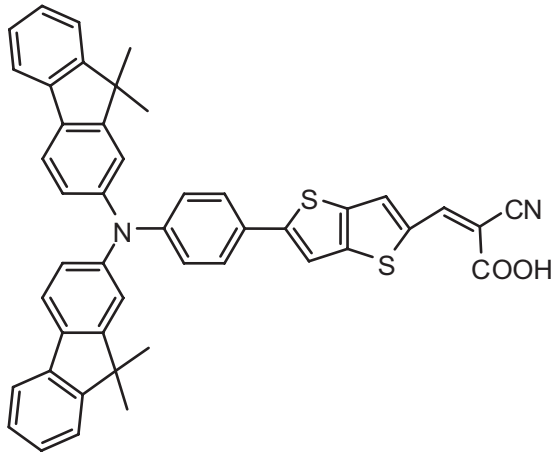

Figure 1. Molecular structure of the C201 sensitizer.

measured LUMO (−0.78 V vs. NHE) of C201 relative to the conduction band edge (−0.50 V vs NHE) of TiO_2 provides a suitable thermodynamic driving force for electron injection even considering the possibly existent exciton binding energy of organic sensitizers. As shown in Figure S1, well-defined anodic and cathodic peaks in the positive potential range both appear at 1.0 V, which is 0.46 V higher than that of the triiodide/iodide redox couple in electrolytes, ensuring a sufficient driving force for efficient dye regeneration and thus net charge separation.

The electronic absorption and emission spectra of the C201 dye in chloroform are shown in Figure 2. The molar extinction coefficients of absorption peaks at 366 and 514 nm are $47.3 \times 10^3\,M^{-1}\,cm^{-1}$ and $41.2 \times 10^3\,M^{-1}\,cm^{-1}$, respectively. We have further observed that in contrast to the insensitivity of high-energy absorption band, the low-energy charge-transfer absorption band of the deprotonated C201 dye was ~76 nm blue-shifted due to the weakened electron-withdrawing strength of carboxylate compared to carboxylic acid. This will be a good preliminary diagnostic tool to know

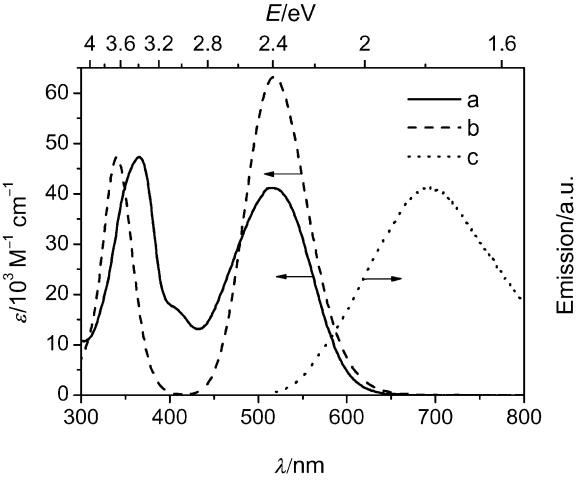

Figure 2. Experimental (a) and calculated (b) electronic absorption and emission (c) spectra of the C201 sensitizer in chloroform.

the protonation/deprotonation status of similar sensitizers, ensuring a correct description of their photophysical and electrochemical behavior. During column purification of these dyes, deprotonation may occur due to the acidity of the 2-cyano-acrylic acid group. Furthermore, the emission of C201 is centered at 692 nm and the excitation transition energy (E_{0-0}) was roughly estimated to be 2.13 eV by taking the crossing-point of its absorption and emission spectra.

The origins of these electronic absorptions are detailed by calculating the singlet electronic transitions with the ZINDO/S method in Gaussian03W program suite. Calculation results show that there are two electronic transition bands of the C201 dye in the UV-vis region (Fig. 2), being well consistent with the experimental data. The visible band at 518 nm is mainly attributed to the electronic transition from the highest occupied molecular orbital (HOMO) to the lowest unoccupied molecular orbital (LUMO) mixed with a perceptible contribution of electronic transition from the next HOMO (HOMO−1) to LUMO. In the C201 sensitizer, HOMO is mainly populated over the triarylamine moiety while LUMO is mainly populated on the anchoring moiety. This orientationally spatial separation of HOMO and LUMO is an ideal condition for dye-sensitized solar cells, which not only facilitates the ultrafast interfacial electron injection from the excited dyes to the TiO_2 conduction band, but also slows down the recombination of injected electrons in TiO_2 with oxidized sensitizers due to their remoteness. In addition, the hole localized on the triarylamine unit will be spatially convenient for the electron donor to approach, facilitating the fast dye-regeneration. Moreover, both HOMO and LUMO have the overlapping extension on the thienothiophene fragment, enhancing the electronic coupling parallel to the electronic transition dipole moment between the two states, which in turn results in a certain oscillator strength between these two electronic states in view of the Frank-Condon principle. All the molecular orbitals involved in the transitions are shown in Figure S2. Detailed assignments for electronic transitions are listed in Table S1.

Preliminary photovoltaic experiments were conducted to evaluate the performance of this C201 dye using a highly volatile acetonitrile based electrolyte, a solvent-free ionic liquid electrolyte or solid-state spiro-OMeTAD[12] as hole transporting materials. The electrolyte compositions of liquid devices were as follows. Electrolyte in device A: 1.0 M 1,3-dimethylimidazolium iodide, 0.05 M LiI, 0.1 M guanidinium thiocyanate, 30 mM I_2, 0.5 M *tert*-butylpyridine in the mixture of acetonitrile and valeronitrile (85/15, v/v); electrolyte in device B: 1,3-dimethylimidazolium iodide/1-ethyl-3-methylimidazolium iodide/1-ethyl-3-methylimidazolium tetracyanoborate/iodine/*N*-butylbenzoimidazole/guannidinium thiocyanate (molar ratio: 12/12/16/1.67/3.33/0.67). State-of-the-art mesoporous double-layer titania film[13] was employed as negative electrode for liquid devices A and B. A 7-μm-thick film of 20-nm-sized TiO_2 particles was first screen-printed on a fluorine-doped SnO_2 (FTO) conducting glass electrode and a 4-μm-thick second layer of 400-nm-sized light scattering

anatase particles was subsequently coated onto the first one. The TiO_2 electrode was derivatized by immersing it into a dye solution containing 300 μM C201 and saturated 3α,7α-dihyroxy-5β-cholanic acid in chlorobenzene at room temperature for ~5 h. A platinized FTO conducting glass was used as positive electrode. The two electrodes were separated by a 25 μm thick Surlyn hot-melt gasket and sealed up by heating. The internal space was filled with the above mentioned electrolytes using a vacuum back-filling system. The electrolyte-injecting hole made in advance by an ultrafine sandblaster on the counter electrode glass substrate was sealed with a Bynel sheet and a thin glass cover by heating. For the solid-state device C, a compact TiO_2 layer was firstly deposited onto the FTO substrate by spray pyrolysis,[14] onto which 20-nm-sized TiO_2 particles were deposited by doctor-blading to obtain a 1.7 μm-thick mesoporous film. After sintering the TiO_2 layers at 500 °C, the film was cooled to room temperature and immersed overnight in 0.02 M aqueous $TiCl_4$. The film was then rinsed with deionized water, annealed in air at 450 °C for 20 min, and cooled to 80 °C before immersing it in the above mentioned dye solution for staining. The hole transporting material solution containing 0.17 M Spiro-OMeTAD, 0.11 mM *tert*-butylpyridine, and 0.21 mM $LiN(CF_3SO_2)_2$ in chlorobenzene was used. We deposited this solution onto the dye-coated TiO_2 film, leaving it penetrate into the pores of the TiO_2 layer for 1 min prior to spin coating. Finally, a 50 nm-thick gold contact was deposited onto the organic semiconductor to close the cell.

The photocurrent action spectrum of device A with C201 as sensitizer is shown in Figure 3A. The incident photon-to-collected electron conversion efficiency (IPCE) exceeds 80% from 450 nm to 580 nm, reaching the maximum of 91% at 530 nm. Considering the light absorption and scattering loss by the conducting glass, the maximum efficiency for absorbed photon-to-collected electron conversion efficiency (APCE) is close to unity over a broad spectral range. As shown in Figure 3B, the short-circuit photocurrent density (J_{sc}), open-circuit photovoltage (V_{oc}), and fill factor (*FF*) of device A with an acetonitrile based electrolyte under an irradiance of AM 1.5G full sunlight are 13.35 mA cm^{-2}, 777 mV, and 0.749, respectively, yielding an overall conversion efficiency (η) of 7.8%. The photovoltaic parameters (J_{sc}, V_{oc}, *FF*, and η) of device B are 12.40 mA cm^{-2}, 723 mV, 0.779, and 7.0%, respectively. This efficiency is impressive for a dye-sensitized solar cell with a solvent-free ionic liquid electrolyte. As depicted in Figure S3, device B shows an excellent light soaking stability at 60 °C. After over 1,000 h aging tests, device efficiency only changed from 6.7 to 6.2%. While there is a 70 mV drop of V_{oc}, the final photocurrent density is even higher than the initial value, proving an extraordinary stability of this all-organic C201 sensitizer in DSC measurements. In addition, the all-solid-state device C with Spiro-OMeTAD as hole-transporting material shows a J_{sc} of 9.06 mA cm^{-2}, a V_{oc} of 860 mV, and a *FF* of 0.61, resulting in an impressive efficiency of 4.8%. This is the first time that such a high efficiency has been reached for all-solid-sate DSCs with a metal-free organic dye.[15] At lower light

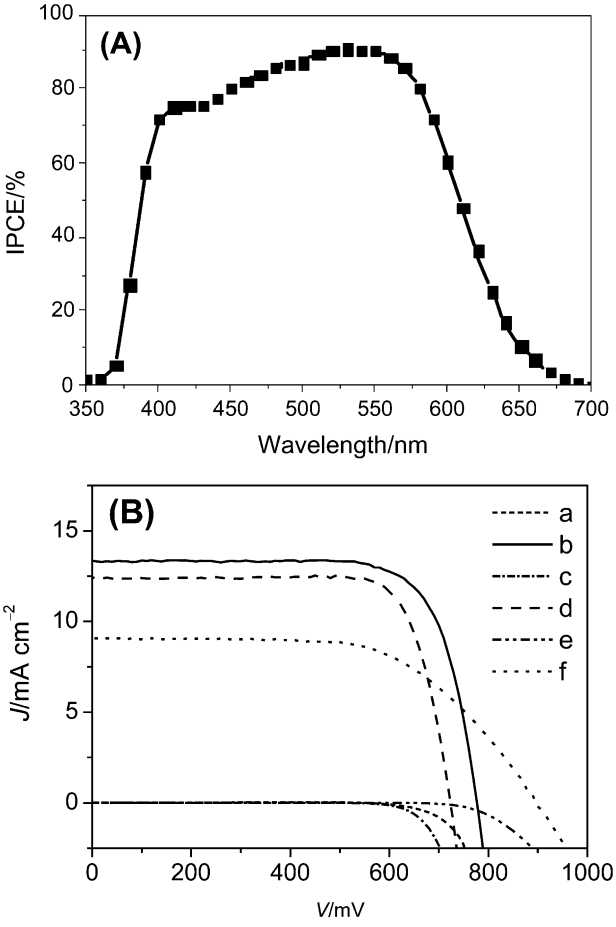

Figure 3. A) Photocurrent action spectrum of device A. B) *J*–*V* characteristics measured in the dark and under an illumination of the AM 1.5G full sunlight (100 mW cm^{-2}). a) device A in the dark; b) device A under light; c) device B in the dark; d) device B under light; e) device C in the dark; f) device C under light. Liquid cells were tested using a metal mask with an aperture area of 0.158 cm^2. Pixel area of solid device: 0.120 cm^2.

intensities, the power conversion efficiencies are over 5%. If a high-reflection silver cathode was used, the performance of this organic dye based solid-state DSC would be enhanced further at full sunlight.[16]

In order to lower the production cost of photovoltaic power, a substantial improvement in device efficiency of DSCs is still desirable. Nevertheless, flexible and light-weight solar cells based on plastic matrix are attractive even if their solar conversion yield is moderate. However, for these devices the use of organic solvents is undesirable, as they would permeate across the polymeric cell walls. Two very attractive solutions to this dilemma consist in employing solvent-free ionic liquid electrolytes or all-solid-state hole transporting materials. Apart from designing more efficient sensitizers and mesoporous films and engineering of the nanointerface between electron- and hole-transporters for further device enhancement, we are curious to understand the origins of relatively lower photocurrent densities of devices B and C compared with A. We measured photoelectrical transients[4,17] to scrutinize

ADVANCED MATERIALS

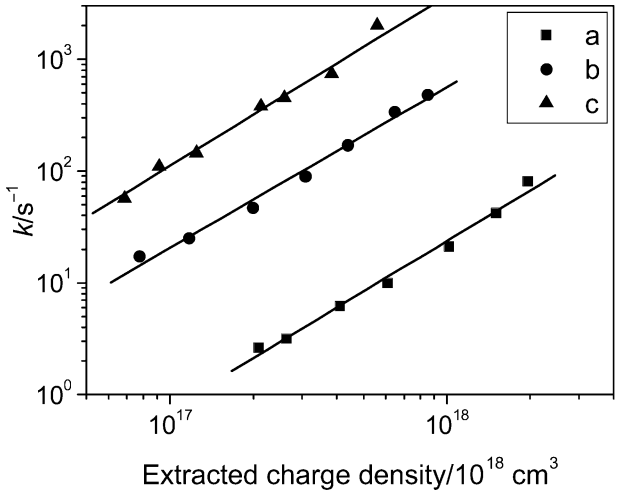

Figure 4. Plots of charge recombination rate constant versus extracted charge density. a) device A; b) device B; c) device C.

the charge recombination at the titania/electrolyte (or solid Spiro-OMeTAD) interface. As shown in Figure 4, along with the increase of extracted charge density from titania films, the recombination rates become higher due to the higher electron densities in the titania film as well as larger driving forces for charge recombination. Obviously, the trend of charge recombination rates (k) of devices A∼C is well consistent with that of the above measured photocurrent densities.

In summary, we have successfully developed a high molar extinction coefficient metal-free sensitizer to realize high performance and applicable dye-sensitized solar cells. Along with a solvent-free ionic liquid electrolyte, we have demonstrated a ∼7% cell with this sensitizer showing an excellent stability measured under the thermal and light-soaking dual stress. Furthermore, for the first time a 4.8% efficiency was reached for all-solid-state dye-sensitized solar cells based on a metal-free organic dye even its spectral response does not match well with the AM 1.5G solar emission. This work will encourage the further systematic research on molecular and energy-level engineering of more efficient all-organic sensitizers for high-performance applicable devices, speeding up the large-scale production and application of flexible thin film organic solar cells.

Received: April 28, 2008
Published online:

[1] M. D. Archer, R. Hill, *Clean Electricity from Photovoltaics*, Imperical College Press, London **2001**.
[2] For a special issue on organic-based photovoltaics see: *MRS Bull.* **2005**, *30*, 10.
[3] Y. Chiba, A. Islam, Y. Watanabe, R. Komiya, N. Koide, L. Han, *Jpn. J. Appl. Phys. Part 2* **2006**, *45*, L638.
[4] F. Gao, Y. Wang, D. Shi, J. Zhang, M. Wang, X. Jing, R. Humphry-Baker, P. Wang, S. M. Zakeeruddin, M. Grätzel, *J. Am. Chem. Soc.* **2008**, *130*, 10720.
[5] M. Pope, C. E. Swenberg, *Electronic Processes in Organic Crystals and Polymers*, 2nd ed., Oxford University Press, Oxford **1999**.
[6] C. W. Tang, *Appl. Phys. Lett.* **1986**, *48*, 183.
[7] H. J. Snaith, L. Schmidt-Mende, *Adv. Mater.* **2007**, *19*, 3187.
[8] a) K. Hara, M. Kurashige, Y. Dan-oh, C. Kasada, A. Shinpo, S. Suga, K. Sayama, H. Arakawa, *New J. Chem.* **2003**, *27*, 783. b) T. Horiuchi, H. Miura, K. Sumioka, S. Uchida, *J. Am. Chem. Soc.* **2004**, *126*, 12218. c) K. Hara, Z.-S. Wang, T. Sato, A. Furube, R. Katoh, H. Sugihara, Y. Dan-oh, C. Kasada, A. Shinpo, S. Suga, *J. Phys. Chem. B* **2005**, *109*, 15276. d) D. P. Hagberg, T. Edvinsson, T. Marinado, G. Boschloo, A. Hagfeldt, L. Sun, *Chem. Commun.* **2006**, 2245. e) N. Koumura, Z.-S. Wang, S. Mori, M. Miyashita, E. Suzuki, K. Hara, *J. Am. Chem. Soc.* **2006**, *128*, 14256.
[9] S. Ito, S. M. Zakeeruddin, R. Humphry-Baker, P. Liska, R. Charvet, P. Comte, M. K. Nazeeruddin, P. Péchy, M. Takata, H. Miura, S. Uchida, M. Grätzel, *Adv. Mater.* **2006**, *18*, 1202.
[10] S. Kim, J. W. Lee, S. O. Kang, J. Ko, J. H. Yum, S. Fantacci, F. De Angellis, D. Di Censo, M. K. Nazeeruddin, M. Grätzel, *J. Am. Chem. Soc.* **2006**, *128*, 16071.
[11] Z.-S. Wang, Y. Cui, K. Hara, Y. Dan-oh, C. Kasada, A. Shinpo, *Adv. Mater.* **2007**, *19*, 1138.
[12] U. Bach, D. Lupo, P. Comte, J. E. Moser, F. Weissörtel, J. Salbeck, H. Spreitzer, M. Grätzel, *Nature* **1998**, *395*, 583.
[13] P. Wang, S. M. Zakeeruddin, P. Comte, R. Charvet, R. Humphry-Baker, M. Grätzel, *J. Phys. Chem. B* **2003**, *107*, 14336.
[14] L. Kavan, M. Grätzel, *Electrochim. Acta* **1995**, *40*, 643.
[15] L. Schmidt-Mende, U. Bach, R. Humphry-Baker, T. Horiuchi, H. Miura, S. Ito, S. Uchida, M. Grätzel, *Adv. Mater.* **2005**, *17*, 813.
[16] H. J. Snaith, A. J. Moule, C. Klein, K. Meerholz, R. H. Friend, M. Grätzel, *Nano Lett.* **2007**, *11*, 3372.
[17] a) B. C. O'Regan, F. Lenzmann, *J. Phys. Chem. B* **2004**, *108*, 4342. b) M. Bailes, P. J. Cameron, K. Lobato, L. M. Peter, *J. Phys. Chem. B* **2005**, *109*, 15429. c) N. Kopidakis, N. R. Neale, A. J. Frank, *J. Phys. Chem. B* **2006**, *110*, 12485. d) A. B. Walker, L. M. Peter, K. Lobato, P. J. Cameron, *J. Phys. Chem. B* **2006**, *110*, 25504. e) M. Quintana, T. Edvinsson, A. Hagfeldt, G. Boschloo, *J. Phys. Chem. C* **2007**, *111*, 1035. f) Z. Zhang, S. M. Zakeeruddin, B. C. O'Regan, R. Humphry-Baker, M. Grätzel, *J. Phys. Chem. B* **2005**, *109*, 21818. g) Z. Zhang, N. Evans, S. M. Zakeeruddin, R. Humphry-Baker, M. Grätzel, *J. Phys. Chem. C* **2007**, *111*, 398.

